Article

Evaluating the Evacuation and Rescue Capabilities of Urban Open Space from a Land Use Perspective: A Case Study in Wuhan, China

Jie Gong [1,2,3], Yaolin Liu [1,2,3,*], Yanfang Liu [1,2,3], Pujiang Huang [4] and Jiwei Li [1,2,3] (iD)

[1] School of Resource and Environmental Science, Wuhan University, 129 Luoyu Road, Wuhan 430079, China; gjie832@163.com (J.G.); yfliu610@163.com (Y.L.); lijiwei19850620@126.com (J.L.)

[2] Key Laboratory of Geographic Information System, Ministry of Education, Wuhan University, 129 Luoyu Road, Wuhan 430079, China

[3] Collaborative Innovation Center for Geospatial Information Technology, Wuhan University, 129 Luoyu Road, Wuhan 430079, China

[4] Shanghai Urban Planning and Design Research Institute, 331 Tongren Road, Shanghai 200010, China; geohuangpj@163.com

[*] Correspondence: yaolin610@163.com; Tel.: +86-027-6877-8552

Abstract: This study proposes an innovative integrated method for evaluating the evacuation and rescue capabilities of open spaces through a case study in Wuhan, China. A dual-scenario network analysis model was set up to calculate travel time among communities, open spaces, and rescue facilities during peak and non-peak hours. The distribution of traffic flow was derived on the basis of a gravity model and used to construct supply-demand indexes (SDIs). SDIs such as evacuation (ESDI), rescue (RSDI), and comprehensive SDIs (CSDI) were used to evaluate the suitability of open space locations. This study drew five major findings as follows: (1) ESDI, RSDI, and CSDI can effectively evaluate the spatial suitability of open spaces when these SDIs are integrated with the gravity model; (2) The quadrant distribution analysis of ESDI can be an effective method for determining the reasons for the change in values in the two traffic scenarios and for helping planners in adjusting their policies to enhance the capability of an area; (3) The impact of the different β values on SDIs can show positive, negative, and inconspicuous correlations with large, moderate, and minimal variations, respectively; (4) The analysis of the supply-demand relationship of open spaces in Wuhan indicates a spatial mismatch in comprehensive evacuation and rescue capacities; (5) Traffic congestion can be a significant impact factor on evacuation and rescue capabilities but not on comprehensive capability.

Keywords: evacuation; rescue; open space; gravity model; supply-demand index; dual-traffic scenario; China

1. Introduction

Cities have been facing threats from natural (e.g., floods, earthquakes, and tsunamis) and man-made (e.g., accidental fires) disasters. These threats may lead to huge losses for densely populated and poorly equipped cities in the developing world. China is among these countries, which are stricken by natural disasters. For example, the 2008 Wenchuan Earthquake hit the densely populated Sichuan Province in China and caused more than 370,000 casualties [1]. The Great Tangshan Earthquake wiped out Tangshan City, claimed 242,000 lives, and caused an overall loss of 5.4 billion yuan in 1976 [2]. The blast of a dangerous chemical warehouse in the Tianjin Binhai New Development Zone was a man-made disaster that led to 159 casualties and 6.866 billion yuan in losses in 2015 [3]. Therefore,

a good understanding of disaster emergency responses can provide important practical value and help to reduce the losses caused by disasters.

Disaster emergency responses involving evacuees, rescuers, government institutions, and social organizations can be divided into two processes; evacuation and rescue (Figure 1). For the evacuation process, studies have focused on evacuation simulation and behavior. Simulation models such as agent-based models [4,5] and least cost distance models [6] help to find the appropriate evacuation route and calculate the evacuation time and costs. Meanwhile, studies on evacuation behavior have concentrated on the responses of individuals during disasters and have examined departure time, vehicle usage, and destination choice. Gravity-based methods and surveys have been widely used in studying the distribution and destination choices of evacuees. Modali [7] and Wilmot [8] implemented improvements in simulating evacuation distribution based on a gravity model. Behavioral science surveys have investigated the changes in the types of destinations and compliance under different conditions. Previous studies have revealed that the proportion of evacuees to the homes of relatives or friends is the largest (54–70.2%), followed by hotels/motels (15.7–29%) and shelters (1–43%) [9–13]. Public shelter is one of the most important destination types in the evacuation process. Compliance during different disasters varies from 11.7% to 97% [14–19].
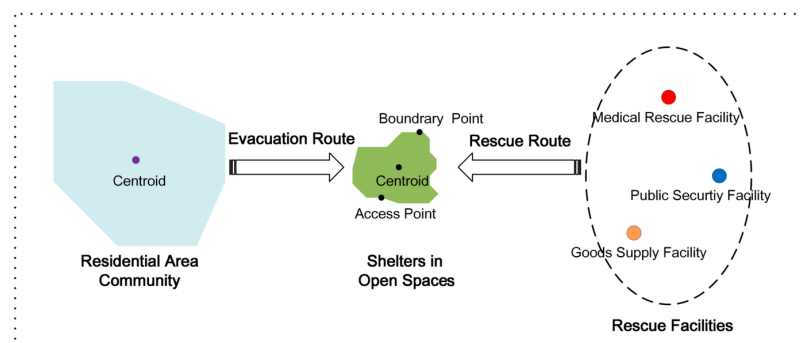

Figure 1. Schematic of evacuation and rescue factors. The evacuation process includes a residential area, shelters, and an evacuation route. The rescue process includes shelters, a rescue route, and rescue facilities for medical purposes, security, or goods supply. Evacuation and rescue constitute disaster responses.

For the rescue process, which is another essential aspect of disaster response, researchers have emphasized searching for or locating evacuees, optimizing networks and routes, and organizing rescue efforts. Many models such as the multi-criteria decision-making method [20], RescueMe [21], and RoboCup Rescue [22] are set up to assist in searching for evacuees. Moreover, scholars have contributed to the methodology for mobilizing resources and selecting safe and efficient routes to disaster areas. For example, Barbarosoglu and Arda [23] used a two-stage stochastic programming model to devise a plan for transporting commodities to disaster areas. Gharakhlou et al. [20] investigated different physical and semi-physical patterns to increase access to different districts. Hu and Sheng [24] adopted a multi-agent system to simulate, assess, and analyze the impact of disasters and rescue time. Wei et al. considered unexpected accidents and used a modified Dijkstra algorithm to obtain the real-time shortest rescue route in a road network [25].

D'Agostino et al. [26], Khamis et al. [27], and Barsky et al. [28] provided significant contributions in the field of rescue management. The design of the rescue capabilities of shelters, including efforts for reducing travel time or distance and enhancing the efficiency of rescue work before disasters occur, has been insufficiently studied, although the important role of rescuing capability during disasters is reflected in these papers.

In addition to conventional measures for controlling hazards, recent studies explore the role of land use planning in reducing exposure to and alleviating the influence of disaster [29,30]. The Chinese

government has been requiring all shelters to be sites that can serve general civil purposes and disaster relief efforts, denoting the construction of open spaces, green land, and squares that meet standards of safety and capability into shelters to maximize land use. This study selected open spaces in urban areas as shelter sites. According to the definition used in previous studies, urban open spaces are safe, well-managed areas, including green spaces (e.g., residential, neighborhood, quarter, district, and city greens and urban forests), sports fields, civic squares, and schools, that can be accessed by the public freely [31–36]. Furthermore, emergency shelters can only provide temporary refuge, medical care, goods, information, and other survival necessities [37]. According to the field survey conducted by this study in Hongshan Square, the first national-level emergency shelter in Wuhan, rescue workers or goods (e.g., food, medicine, and medical equipment) were unavailable in the shelter during a non-emergency period.

Existing studies have been limited on several fronts, despite the progress in understanding disaster emergency responses. First, early studies mainly focused on evacuation and rescue alone, thereby leaving a gap in the quantitative model combining evacuation and rescue to assess public shelter capability, particularly from a land use perspective. Second, scholars adopt evacuation time and the population size of the evacuees to reach a safe place within a certain time as indicators for measuring the evacuation capability of a city. However, the spatial distribution of shelters and the balance between resource availability and demand should be considered. An index that denotes the relationship between supply and demand should also be established.

Therefore, this study aims to provide a theoretical and comprehensive supply-demand index (CSDI) to evaluate the quantity and spatial layout of open spaces to indicate disaster evacuation and rescue capabilities at the city level. The remainder of this paper is organized as follows. Section 2 describes the study area and data sources. Section 3 discusses the methods used. Then, Section 4 provides the results and interpretations. Section 5 presents the discussion. Finally, Section 6 delivers a summary and suggests potential directions for future research.

2. Materials

2.1. Study Area

City disaster defense management had become a crucial issue in China since the 2008 Wenchuan Earthquake occurred. The Standards of Earthquake Emergency Shelter and Related Facilities [38] were published, and many cities started to conduct disaster defense planning. Wuhan is one of these cities. Five major disasters, including floods, geological disasters, fires, explosions, and industrial disasters, were identified. Simultaneously, the planning of a comprehensive disaster prevention method and shelter in the Wuhan Urban Development Area was established [39]. However, a quantitative measurement of whether open spaces are reasonably distributed as disaster shelters is still lacking.

Wuhan is the capital of Hubei Province and is an important hub for the water, land, and air transportation of Central China as depicted in Figure 2. Wuhan is a rapidly growing city, and many people are attracted to residing in this city. In 2012, the main urban area of Wuhan, which is our study area, covered a total area of 960.09 km^2 and recorded a population of 4.96 million. The suburban area of Wuhan is excluded from this study because of its rural landscape and land use and low population density.

The Yangtze and Han Rivers split the main urban area of Wuhan into three parts; Wu Chang, Han Kou, and Han Yang. Three ring roads were built to link the three parts and aimed at easing traffic jams similar to other metropolises in China. Three traffic ring roads divide the entire city into four ring areas. Ring areas 1 to 4, including inner and outer areas, were denoted as the core (RA1), the inner ring (RA2), the outer ring (RA3), and the urban fringe areas (RA4).

The adoption of each ring area as a unit to compare the values of the supply-demand indexes (SDIs) is reasonable because the population, road densities, and the number or size of the open spaces vary significantly among the ring areas, as illustrated in Figures 3 and 4.
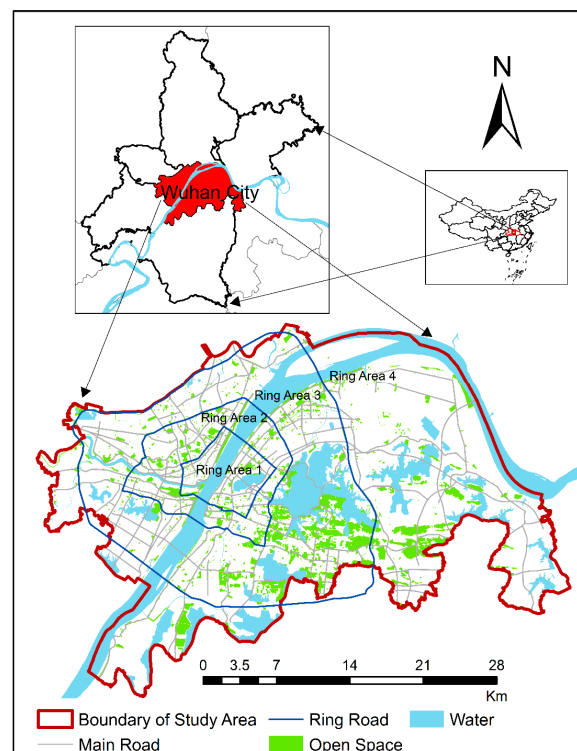
Figure 2. Case study area in the main part of Wuhan City in China with open spaces, water, four ring roads, and main roads.
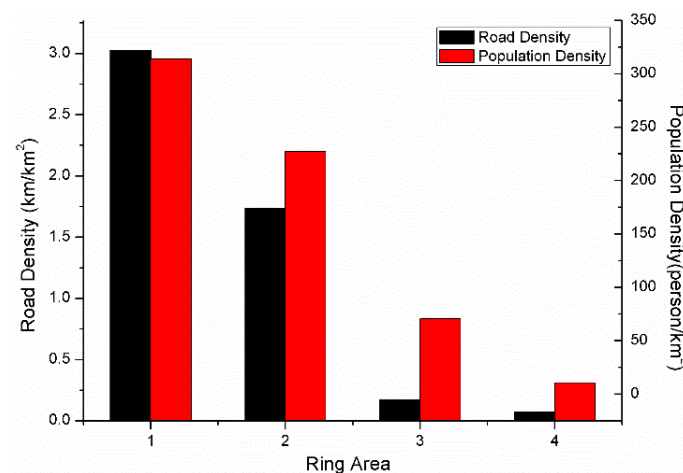

Figure 3. Density of road and population in each ring area.

2.2. Data

Land use data and community boundaries in 2012 were obtained from the Wuhan Urban Planning Bureau. In this study, community refers to the fifth level of the administrative region unit in an urban area, which has six levels in the order of province, city, county, township, community, and group [40]. One community generally contains 1000 to 3000 households [41]. A community tract refers to a community administrative region projected onto the map. Land use data include the location and types of open spaces, facilities, and roadway networks. A series of data preprocessing was conducted to obtain the fundamental data of this research, considering suitability, safety, acquirable data, and accuracy.
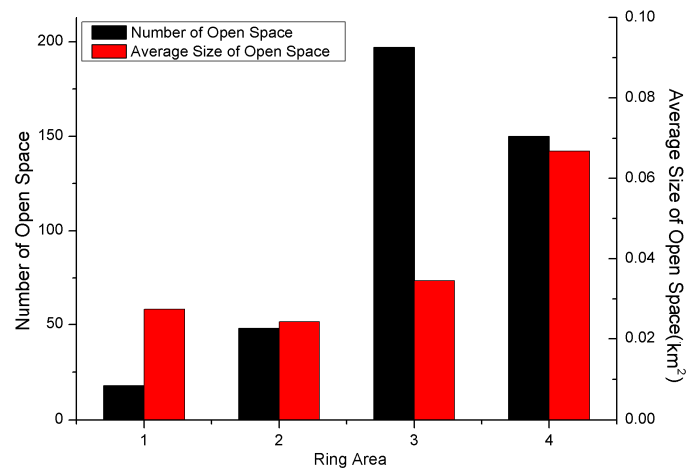
Figure 4. Number and size of open space in each ring area.

The suitability and security of all open spaces in Wuhan were assessed on the basis of the Chinese standards for selecting emergency shelter sites [38]. The following criteria were selected as the principles of safety assessment:

1. The total area of the open space should be larger than 1 km^2.
2. The effective area of the open space, that is, the area of the open space that excludes the land covered by buildings and large plants or other unsuitable areas for evacuees to live in and that is determined via field survey, should be larger than 2000 m^2.
3. The open space should not be a flood-prone area.
4. The open space should not be in urban geological disaster areas.
5. The internal slope of the open space should not be greater than 7°.
6. The open space should have at least one road of more than 12 m in length.
7. The shortest distance between open spaces and surrounding high-rise buildings should not be less than the buildings' height(s).
8. Refueling stations, gas facilities, and hazardous chemical enterprises should not be located within a 1 km range of the alternative plot.

A total of 414 urban open spaces were considered suitable refugee shelters, with a total area of 39.51 km^2 and an effective shelter area of 18.60 km^2. The distribution of open spaces is illustrated in Figure 5a.

The public service facilities related to disaster rescue included 183 medical rescue, 75 public security maintenance, and 43 goods supply facilities. The capabilities of the medical rescue and public security maintenance facilities, excluding the capability of the goods supply facilities of the city in 2012, which was obtained from the Wuhan Urban Planning Bureau, were measured on the basis of published standards for many megacities in China [42–46] (Table 1).

Table 1. Service Capacity Standard for Public Rescue Facilities.

Rescue Facilities	Service Capacity (in Persons)
Medical rescue facility	
Comprehensive hospital	120,000
Specialized hospital	60,000
Community hospital	20,000
Security maintenance facility	120,000
Goods supply facility	80,000

(a) Open spaces and public rescue facilities

(b) Population and communities

(c) Road speeds during non-peak hours
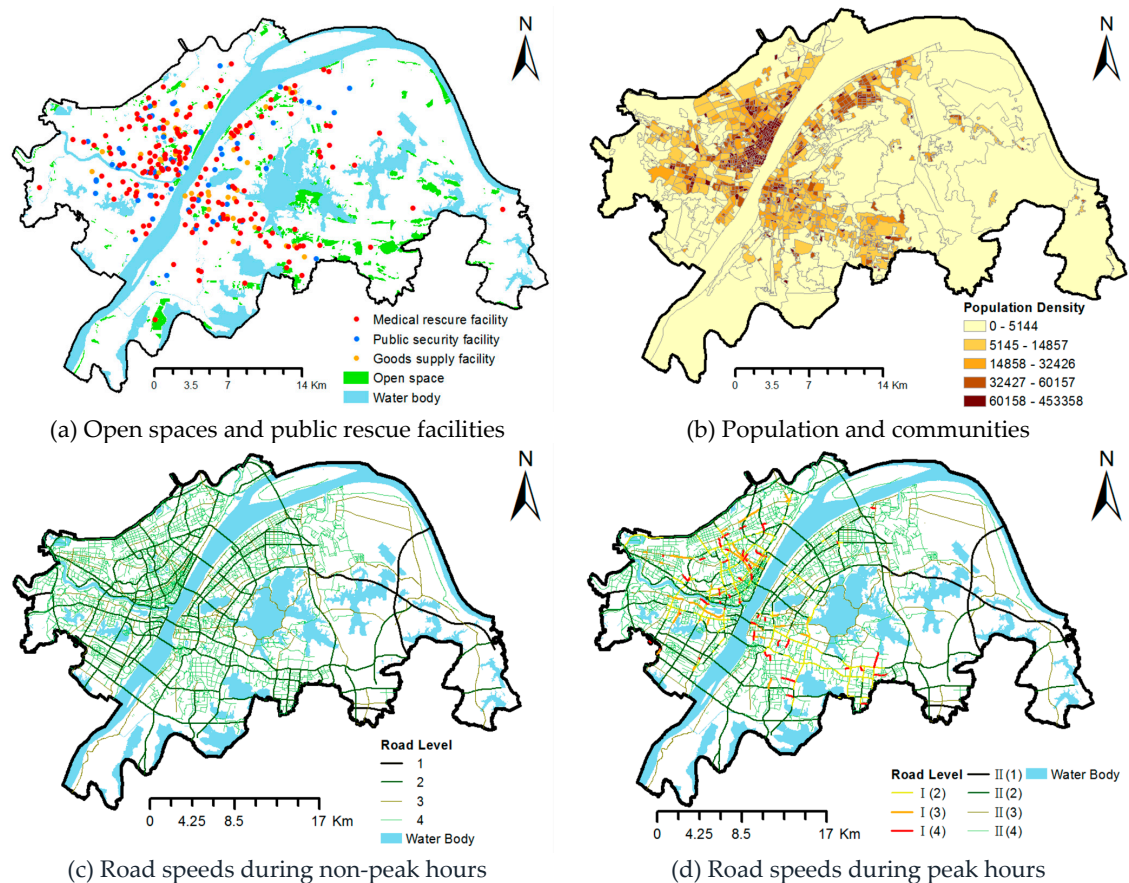

(d) Road speeds during peak hours

Figure 5. Spatial data utilized in the analysis. (**a**) Screened open spaces adopted and the distribution of public security, medical rescue, and goods supply facilities; (**b**) A total of 1071 communities with their population densities; (**c**) Road speeds during non-peak hours. The road levels represent different hierarchies; Level 4 denotes a paved road, Level 3 a branch road, Level 2 the general road, and Level 1 the main road; (**d**) Road speeds during peak hours. I represents blocked roads. II represents unobstructed roads. Road levels represent different hierarchies; Level 4 denotes paved roads, Level 3 branch roads, Level 2 the general road, and Level 1 the main road.

A reasonable speed was assigned to each road segment at different times according to a 50-week transportation survey conducted by the Wuhan Institute of City Traffic Development and Strategy Research in 2011 and 2012 [47]. During non-peak hours, the speed of vehicles was assigned the design speed of the road in the area excluded by the survey or the actual average driving speed in the area covered by the survey. During peak hours, the speed of vehicles on congested roads was assigned the actual average speed, whereas the speed of vehicles on uncongested roads was assigned the actual average driving speed in the same road hierarchy. The walking speed of pedestrians was the same value in the two traffic background levels (Table 2).

Table 2. Road Types with Their Widths and Speed Limits (unit: km/h).

Hierarchy	Effective Width (m)	Segments	Vehicle Speed		Walking Speed
			Non-Peak Hours	Peak Hours	
Main Road	>15	1569	50	25.5	5
General Road	12–15	753	40	20.8	5
Branch Road	8–12	3976	30	15	5
Paved Road	<8	4134	20	10	5

The population data of the 1071 communities based on the 2010 census were obtained from the Wuhan Census Bureau. This study adopted communities as the evacuation origins because community was the smallest unit for which population data were available as illustrated in Figure 5b.

Wuhan comprises 12,369 road segments. A road segment refers to a section of road between two junctions. This study adopted the method of Zhang et al. to differentiate between the possible security roads, considering the probable building collapses that might occur during a disaster [48]. A total of 10,433 were selected (Figure 5c,d) and classified into different hierarchies based on different effective road widths (Table 2).

3. Methods

3.1. Dual-Scenario Network Analysis Model

Two traffic scenarios were designed, and a dual-scenario network analysis model was established to calculate the evacuation and rescue traffic time from the community (or rescue facilities) to open spaces during peak and non-peak hours.

In the post-disaster response, the traffic subjects, which are subjects that are required to be moved or transported on the road, in the evacuation process were the pedestrians and vehicles. Cars are generally used as the main carriers for delivering aid, workers, and supplies. Therefore, vehicles were adopted as the principal traffic subjects in the rescue process. The network analysis modules in ArcGIS 10.2 were used to find the path that consumes the minimum traffic time $C_{O_iD_j}$ between an origin and a destination.

The points used to represent the origin and destination influence the results of accessibility calculation and should be carefully considered [49]. Higgs et al. adopted boundary points, access points, and centroids as representatives of green space polygons. Boone et al. proposed that the centroids of a polygon can represent small parks and that access points can represent large parks [50]. They also suggested that any point along the perimeter can serve as a representative for a large park. In this study, the open spaces without fences were represented by the nearest Euclidean point on the boundary. The nearest access points denote the locations of open spaces with fences [49]. Communities and rescue facilities were represented by geometric centroids.

Distance is the main index used to measure spatial segregation. It is usually expressed in two ways, Euclidean and network distances, in urban areas. In evaluating the accessibility of open spaces in the urban context, La Rosa indicated that network distance is more precise than Euclidean distance [51]. This study applies the gravity model to calculate the traffic flow between each origin to each destination, considering the possibility mentioned by Kincses and Toth [52]. The present study specifically adopted the time consumed on the road network as a decay parameter, the evacuation and rescue capabilities of open spaces or facilities as public products, and the evacuees or rescuers as customers to determine the travel methods of evacuees and rescuers after a disaster.

This study proposed a dual-scenario network analysis model expressed as:

$$C_{O_iD_j} = min \sum\nolimits_{k=1}^{z} l_k / v_k \tag{1}$$

where $C_{O_iD_j}$ is the minimum time consumed traveling from the origin O_i to the destination D_j, l_k is the length of path k in the network, and v_k is the speed of various traffic subjects under different traffic situations on path k (e.g., person or vehicle speed on each road level during peak or non-peak hours).

This study focused on measuring the spatial relationship between origins and destinations. The accurate simulation of the evacuation rescue process is beyond the scope of this study.

3.2. Gravity Model Based on Evacuation and Rescue Flow Distribution

The gravity model is confirmed by the "first law of geography"; things that are close to one another in space are more related [52]. Spatial flow analysis is one of the basic areas of applying gravity models; this approach calculates the probability of the generated flow between two sites [53] and is

widely used in assessing public facility accessibility [54–57]. For the movement between origin *i* and destination *j*, denoted as Z_{ij}, the simplest form of the gravity model is expressed as:

$$Z_{ij} = C_i P_j f(d_{ij}, \beta) \tag{2}$$

where P_j and C_i represent the observed origin and destination based factors, respectively, and $f(d_{ij}, \beta)$ describes the interaction between *i* and *j* as a decreasing function of distance d_{ij}, parameterized by β.

The three basic factors in the equation are attraction, distance, and damping coefficients.

Attraction is determined by area, facility size, or population. Significant attraction equates to a strong relationship between two sites. Large open spaces likely include additional facilities and large service areas and are likely to be a destination for evacuees. Each open space within certain reachable areas can be selected as an evacuation or rescue destination. Inversely, one public rescue facility can serve multiple open spaces within the surrounding area. The principal attraction factors considered in the gravity model are the capacity of an open space to accommodate evacuees, the number of evacuees in the community, and the service capability of rescue facilities.

The calculation model presented in the subsections was implemented in MATLAB 2012 (MathWorks, Inc., Natick, MA, USA).

3.2.1. Formula of the Gravity Model

$$G_{ij} = N_i M_j / C_{O_i D_j}{}^{\beta} \tag{3}$$

$$M_j = A_i / (a_j + V_c V_a / V_p) \tag{4}$$

where G_{ij} represents the interaction between points *i* and *j* and the probability of the function flow between these points. N_i is the residential population or the service capability of the *i*th community or public rescue facilities. This study used the compliance value of 97%.

Equation (4) calculates the number of evacuees that can be accommodated in *j*th open space. M_j is the number of evacuees that can be accommodated in the *j*th open space. A_i denotes the size of the *j*th open space that the evacuees or rescuers reach. The denominator calculates the average area per person or per vehicle. V_a is the average area occupied by each vehicle and is 15 m^2. V_c denotes the percentage of evacuees who may select riding a vehicle based on the car ownership ratio, which is 15.5%. This study considers that 62% of citizens would ride a vehicle to the shelter. V_p denotes the number of persons each car could carry. This study assumes that each car has four people. a_i is the refuge area, set at 2 m^2, required for each evacuee [38]. β represents the distance damping coefficient that can be expressed by a different mathematical expression. The β value is widely discussed [54,55,58,59]. The variation range of the SDIs of different β values was determined to be (1, 3) (interval of 0.2) to further illustrate the influence of geospatial and transport facilities on the model results and to clearly show multiple results. The SDIs of $\beta = 2$ were clarified particularly in Section 4, and the effect of β value variation was discussed in Section 5.

3.2.2. Evaluation Formula for Evacuation Traffic Flow

The model aggregated the generated traffic function flow between two points into each open space. Then, this flow was used as the supply (demand) value of each point. Evacuation and rescue procedures comprised different supply and demand objects.

In the evacuation process, the demand or supply was the community or open space as expressed in Equations (5) and (6), respectively:

$$ED_j = \sum_{\theta=1}^{t} S_{ij} \times R_{\theta} \tag{5}$$

$$ES_j = M_j \tag{6}$$

where ED_j represents the demand for accommodation based on the number of evacuees; S_{ij} is the value of G_{ij} after maximum difference normalization transformation; R_θ is the residential population of the θth community; and ES_j is the number of evacuees that the jth open space can accommodate.

3.2.3. Evaluation Flow for Rescue Traffic Flow

By contrast, the demand and supply sides in the rescue process were the urban open space and public rescue facilities as expressed in Equation (7).

$$RS_j = \sum_{\delta=1}^{w} S_{ij} \times F_\delta \tag{7}$$

where RS_j is the number of evacuees who could receive rescue services in the jth open space, S_{ij} is the maximum difference standardized value of G_{ij}, and F_δ is the supply capability of the wth rescue facility.

According to the number of citizens who can reach the jth open space within or beyond its capacity, RD_i performs different functions as expressed in Equation (9):

$$RS_j = \sum_{\delta=1}^{w} S_{ij} \times F_\delta \tag{8}$$

$$RD_j = \begin{cases} M_j, & (ED_j > M_j) \\ \sum_{\theta=1}^{t} S_{ij} \times R_\theta, & (ED_j < M_j) \end{cases} \tag{9}$$

where RD_j pertains to the demand of refuge seekers in the jth open space.

3.2.4. SDI

Evacuation supply-demand index (ESDI), rescue supply-demand index (RSDI), and CSDI were established based on traffic flow. SDIs can be measured by utilizing the following equations:

$$\mathrm{ESDI}_j = ES_j / ED_j \tag{10}$$

or

$$\mathrm{RSDI}_j = RS_j / RD_j \tag{11}$$

$$\mathrm{CSDI}_j = w_{ej}\mathrm{ESDI}_j + w_{rj}\mathrm{RSDI}_j \tag{12}$$

where ESDI_j or RSDI_j is the ESDI or RSDI of the jth open space, CSDI_j represents the CSDI of the jth open space, w_{ej} refers to the weight value of ESDI_j, and w_{rj} refers to the weight value of RSDI_j. CSDI is a comprehensive index that can reflect the evacuation and rescue capabilities of open spaces, including their accessibility, supply, and demand.

4. Results

4.1. ESDI

The spatial distribution of the ESDI of the open spaces presented a ring variation tendency under peak and non-peak hours of traffic conditions (Figure 6). The value increased from the core urban area to the urban fringe. The average values of the ESDI of open spaces in RA1–RA4 distinctly varied by distance increasing from the urban center under the two conditions (Figure 6). The average value of open spaces in the RA1 was 0.99 during peak hours, whereas several high values emerged during non-peak hours, which were marked by red spots, with an average value of 2.6. In Figure 7, the average value of each RA is higher during non-peak hours than during peak hours. This phenomenon was

significant in RA1 and RA2, reaching 2.63 and 1.6 times, respectively, indicating that RA1 and RA2 were the areas most severely influenced by the traffic background level. The ESDI maximum value appeared in RA4 in each condition. Two possible reasons can be attributed to this scenario: First, the large supply and insufficient demand for open spaces were in the region of RA4. Second, RA4 is distant from the densely populated areas RA1 and RA2 (Figure 3); thus, RA4 only requires a few external evacuees to be received. In contrast to the case for peak hours, a minimum value of 2.28 during non-peak hours was observed in RA3. It is observed in the model that the open spaces located in RA3 accept more evacuees during non-peak hours than during peak hours. These evacuees could only seek shelter in RA1 and RA2, usually blocked by traffic congestion during peak hours. More than half of the ESDIs are larger than one, according to the normal distribution curve (Figure 8). The non-peak curve is slightly smoother than the peak curves, implying that citizens appreciate equality in shelter resources. The peak curve (μ = 0.17) becomes closer to the line (x = 0) than the non-peak curves (μ = 0.24), indicating that the value is generally lower during peak hours than during non-peak hours.
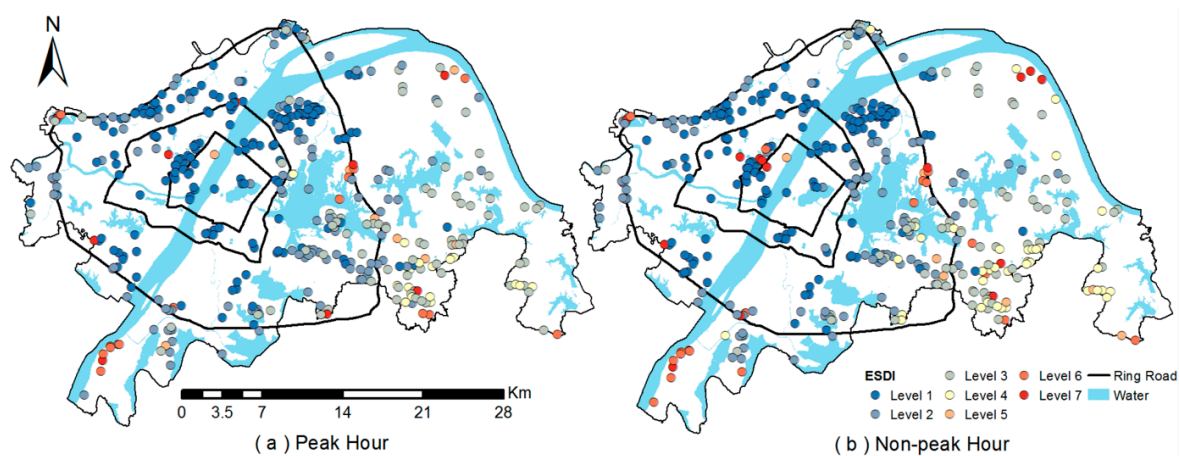

Figure 6. Evacuation supply-demand index (ESDI) distribution. (**a**,**b**) ESDI during peak and non-peak hours, respectively. Level 1: ESDI value range (0–1); Level 2: ESDI value range (1.01–3); Level 3: ESDI value range (3.01–6); Level 4: ESDI value range (6.01–9); Level 5: ESDI value range (9.01–12); Level 6: ESDI value range (12.01–15); and Level 7: ESDI value range (15.01–49.11). The low level equates to the great pressure of supply and demand and the weak evacuation capacity. Level 7 has the strongest evacuation capability, whereas Level 1 has the weakest evacuation capability as supply totally falls short of demand.
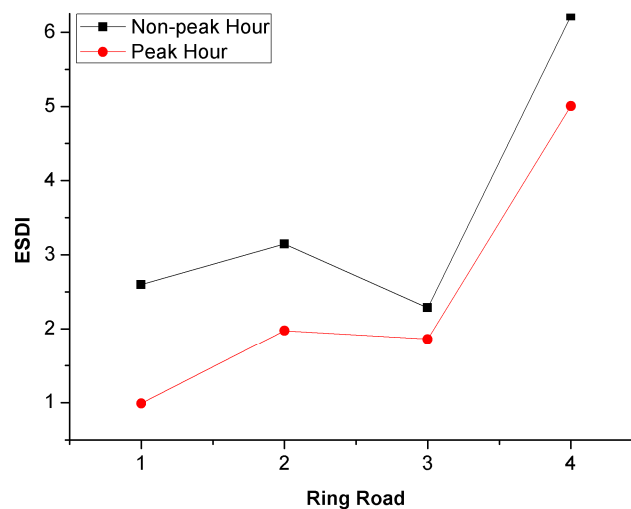
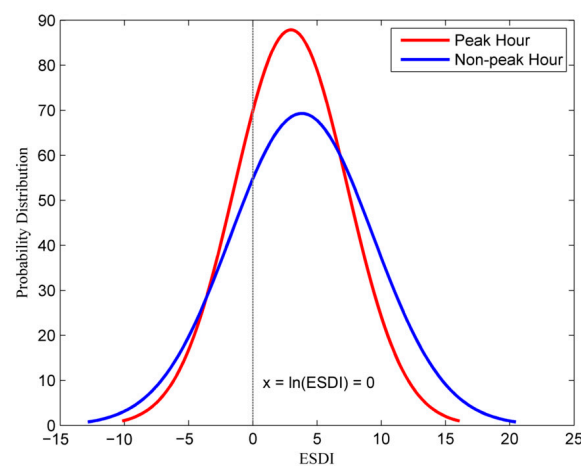

Figure 7. Average ESDI of the ring area.

Figure 8. Normal distribution curve of ESDI.

The number of open spaces with an ESDI value less than one, which is a perfect condition that signifies equal supply and demand, was calculated. The number of overloaded open spaces during peak hours was 169, which comprises 40.92% of the total. By contrast, the number of overloaded open spaces during non-peak hours was 156, which represents 37.77% of the total. The dynamic traffic conditions and the attraction of communities toward open spaces significantly influenced the evacuation capability of the city.

An interesting phenomenon was identified; certain open spaces had preferable ESDI during peak hours compared to non-peak hours. This finding contradicts the previous findings that ESDIs during non-peak hours were preferable to those during peak hours. A scatter diagram (Figures 9 and 10) was adopted to illustrate the values of the two traffic scenarios. The horizontal axis is the index value during peak hours, and the vertical axis is the index value during non-peak hours. The origin of the coordinate is 1. The index shown in the figures only ranges from 0 to 2.

The first quadrant represents the supply that can satisfy the demand. The second quadrant indicates that open spaces are sufficiently supplied during non-peak hours but insufficiently supplied during peak hours. These points can be referred to as Type 1 error points. In the third quadrant, the supply capacity of the shelter cannot satisfy the evacuation demand in the two traffic background levels. The points in the fourth quadrant are Type 2 error points because they have low values during non-peak hours but have values higher than one during peak hours.
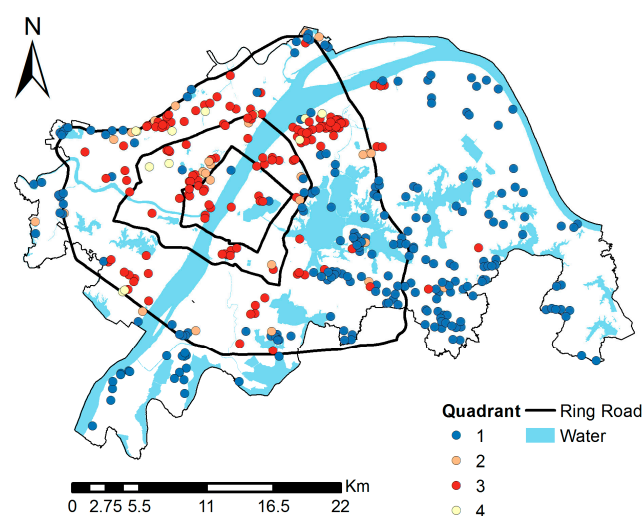

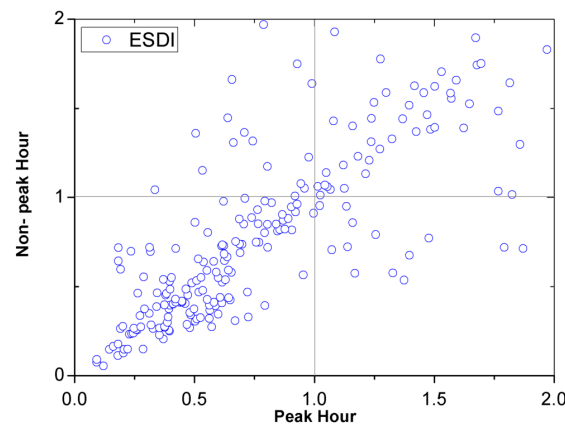**Figure 9.** Quadrant spatial distribution of ESDI.

Figure 10. Quadrant spatial distribution of ESDI.

The points located in Quadrants I and III comprise a large proportion of the total; 55.56% and 34.3%, respectively. Among the points in Quadrant I, RA4 occupies 60% (the most) and RA1 occupies 0.08% (the least). In Quadrant III, RA3 accounts for 61.27% (the most) and RA4 accounts for 4.93% (the least). Quadrants II and IV are nearly completely occupied by the points located in RA3 and RA2. In Quadrant II, RA3 accounts for 48.15%, followed by 29.63% in RA2. In Quadrant IV, RA3 accounts for 71.43%, followed by 28.57% in RA2 (Table 3). A possible reason for the dramatic change in the line in RA3 during non-peak hours is depicted in Figure 8.

Table 3. Proportion of Open Space belonging to Each Quadrant in the Ring Area.

	Total	Quadrant I		Quadrant II		Quadrant III		Quadrant IV	
Total	414	230	55.56%	27	6.52%	142	34.30%	14	3.62%
RA1	17	2	11.76%	1	5.88%	15	88.24%	0	–
RA2	48	3	6.25%	8	16.67%	33	68.75%	4	8.33%
RA3	199	87	43.72%	13	6.53%	87	43.72%	10	6.03%
RA4	150	138	92.00%	5	3.33%	7	4.67%	0	–

4.2. RSDI

The analytic hierarchy process method [60] was used to determine the weights of the rescue factors, which were 0.5006, 0.2746, and 0.2248 for medical rescue, public security maintenance, and goods supply facilities, respectively.

RSDI exhibited a nearly diametrically opposite distribution when compared with ESDI. The value decreases while the distance increases from the inner city to the fringe, as illustrated in Figure 11. Each value of RSDI in the two traffic scenarios was greater than 1, indicating that Wuhan City possesses sufficient rescue capabilities. Figure 12 depicts a RSDI average value that is highest at 13.38 and 12.82 in RA2 during peak and non-peak hours, respectively, followed by RA1 and RA3. RA4 demonstrates the lowest RSDI average value. Figure 13 illustrates that the non-peak hour curve ($\mu = 0.62$) is closer to the line ($x = 0$) than the peak hour curve ($\mu = 0.71$), indicating that Wuhan has sufficient rescue capacity even during peak hours.
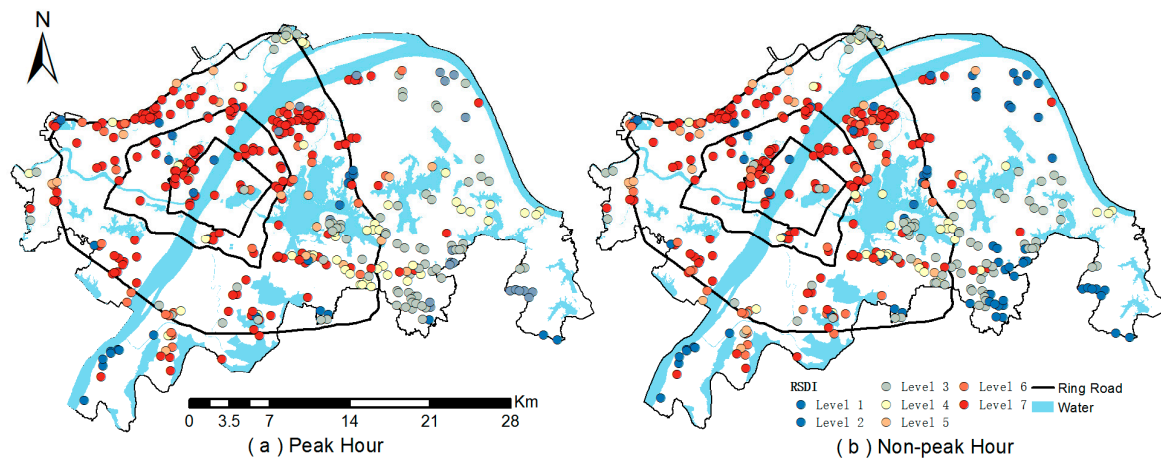
Figure 11. Rescue supply-demand index (RSDI) distribution. (**a**,**b**) RSDI during peak and non-peak hours, respectively. Level 1: RSDI value range (0–1); Level 2: RSDI value range (1.01–2); Level 3: RSDI value range (2.01–3); Level 4: RSDI value range (3.01–4); Level 5: RSDI value range (4.01–5); Level 6: RSDI value range (5.01–6); and Level 7: RSDI value greater than 6. Level 1 indicates that the rescue supply falls short of the rescue necessities of evacuees in open spaces, whereas Level 7 indicates that the rescue capability can fully meet the comprehensive demands of evacuees for health, safety, and goods.
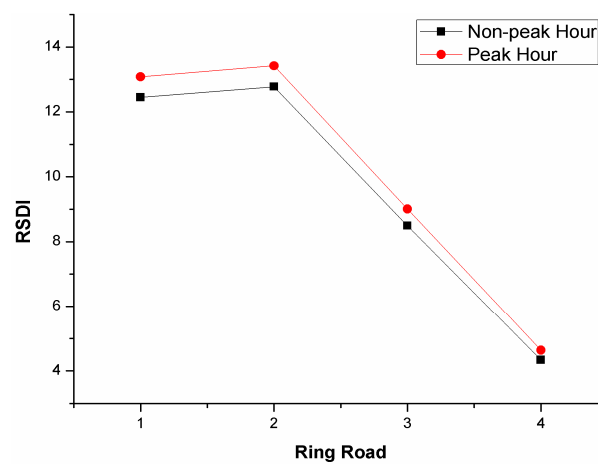

Figure 12. Average RSDI of the ring area.
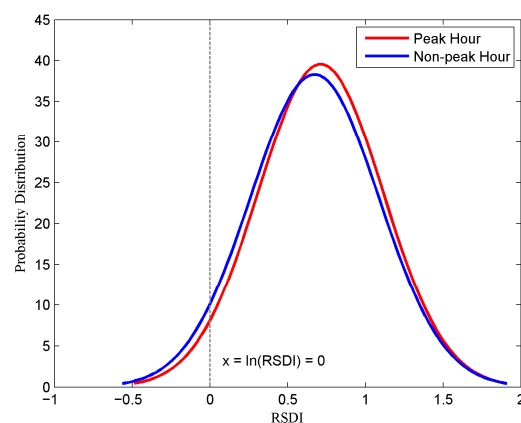

Figure 13. Normal distribution curve of rescue supply-demand index (RSDI).

Among the three specific types of rescue facilities (Table 4), the RSDIs were greater in medical rescue facilities, at 18.57 and 17.65 during peak and non-peak hours, respectively, than in goods supply and public security facilities. Goods supply facilities were under the most pressure in Wuhan, because their values were less than 1. No noteworthy distinction between peak and non-peak hours of goods supply capability was observed. Similar to RSDI, the open spaces located in RA2 performed the best, followed by RA1, RA3, and RA4.

Table 4. Rescue Supply-Demand Index (RSDI) of Each Type of Rescue Facility.

	Public Security Facility		Goods Supply Facility		Medical Rescue Facility	
	Peak hours	Non-peak hours	Peak hours	Non-peak hours	Peak hours	Non-peak hours
RA1	0.29	0.28	3.77	3.49	24.28	23.15
RA2	0.44	0.45	4.56	4.24	24.52	23.37
RA3	0.19	0.18	2.64	2.46	16.71	15.76
RA4	0.07	0.08	1.02	0.93	8.77	8.21

4.3. CSDI

The weights of ESDI and RSDI calculated through the analytic hierarchy process method were 0.5498 and 0.4501, respectively [60]. A significant difference could be noted in Figures 6, 11 and 14. The CSDI spatial distribution trend was insignificant and is generally homogeneous only with several spatial agglomerations.
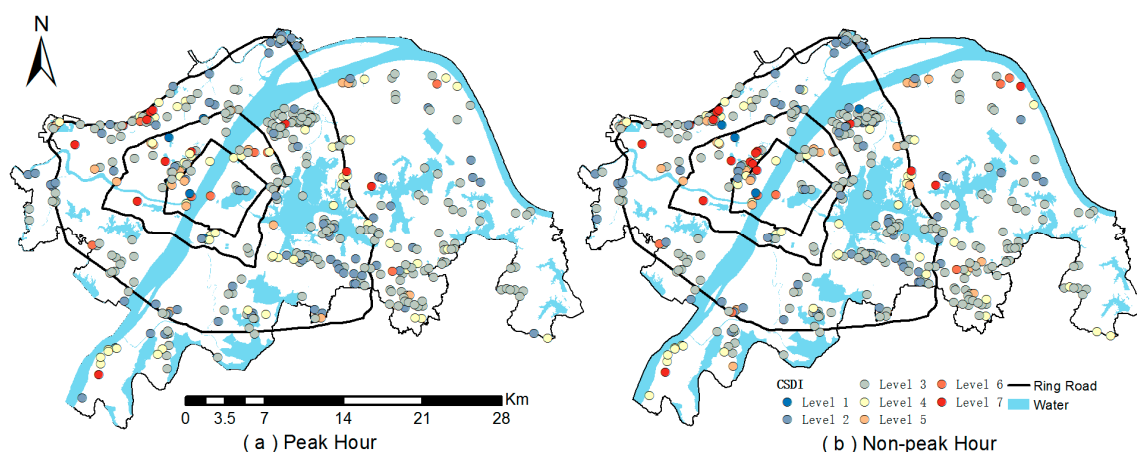

Figure 14. Comprehensive supply–demand index (CSDI) distribution. (**a**,**b**) CSDI during peak and non-peak hours, respectively. Level 1: CSDI value range (0–1); Level 2: CSDI value range (1.01–3); Level 3: CSDI value range (3.01–6); Level 4: CSDI value range (6.01–9); Level 5: CSDI value range (9.01–12); Level 6: CSDI value range (12.01–15); and Level 7: CSDI value greater than 15. CSDI gradually increased from Levels 1 to 7, representing greater evacuation and rescue capabilities. Level 1 represents the weakest capability, whereas Level 7 represents the strongest capability.

RA2 was the safest area in Wuhan, possessing the highest CSDI (CSDI = 7.13 and 7.48 during peak and non-peak hours, respectively), followed by RA1 at 6.43 and 7.03 during peak and non-peak hours, respectively, and then RA3. Although the average CSDI was slightly larger in RA4 than in RA3 during non-peak hours, the CSDI of RA4 during peak hours had the lowest value among all ring areas, making RA4 the weakest area for disaster response (Figure 15). Improvements in road network building or traffic management could be helpful in enhancing security in RA4 because of the area's sensitivity to the traffic background level. During peak hours, the entire city was interspersed with high-value points and one prominent cluster in RA3. During non-peak hours, a new high-value cluster was observed around the first ring road. Virtually all CSDIs were larger than 1 because the normal

distribution curves of peak and non-peak hours were on the right side of the line ($x = 0$). However, no theatrical variation was observed between the two traffic background levels (Figure 16).
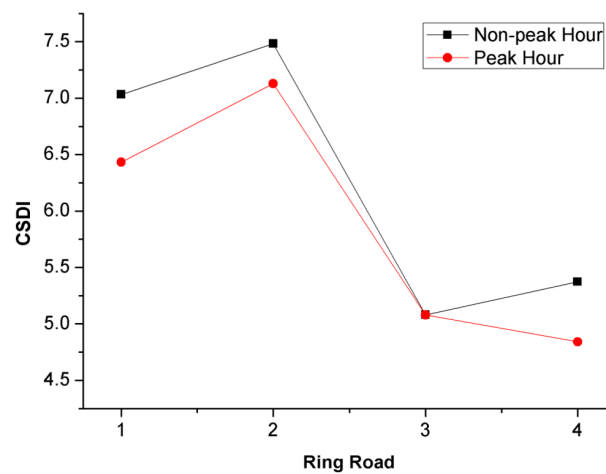

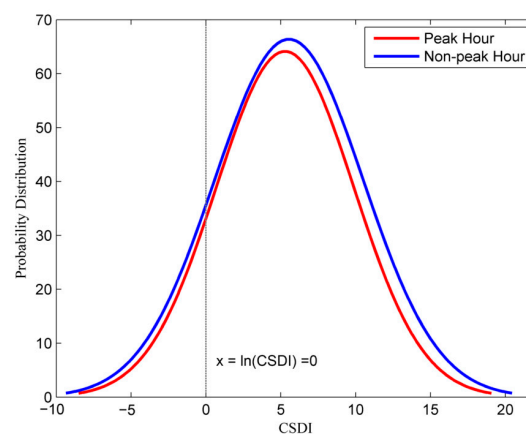**Figure 15.** Average CSDI of the ring area.

Figure 16. Normal distribution curve of CSDI.

5. Discussions

Different β values exhibited different influence directions and degrees of SDI, as illustrated in Figure 17. The results could probably be divided into three categories, as follows. (1) Positive correlation with a large variation: this phenomenon mainly occurred in evacuation and rescue resource-rich areas such as RA4/RA3, with large open spaces in the evacuation process, and RA1/RA2, with considerable resources in the rescue process. A large β value implied that evacuees or rescuers were discouraged by long travel times in seeking open spaces and proceeded instead to open spaces nearby; (2) Negative correlation with a moderate variation: the noteworthy areas, which were only partially self-sufficient and relied on external resources to supply the requirements of the region, were RA2 and RA3 in the evacuation and rescue processes, respectively. Therefore, the increase in traffic resistance could affect the delivery of supply, resulting in a decline in the supply and demand ratio; (3) Inconspicuous correlation with a small variation: the representative areas were RA1 and RA4 in the evacuation and rescue processes, respectively. These regions were supplied deficiently and were far from the supplying resource-rich areas. Therefore, the impact on SDIs was not as significant as in other regions, although traffic resistance increased.
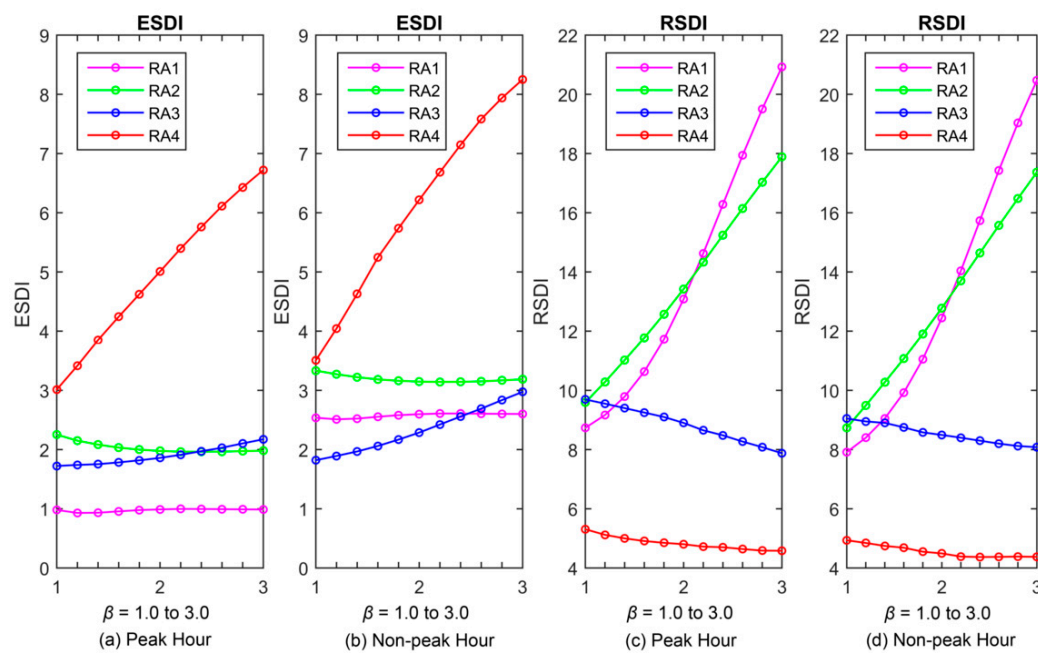
Figure 17. Variation of the average values of ESDI and RSDI under different β values of different ring areas.

The ESDI average value of RA4 was the maximum and most variable among all β values of the two traffic background levels in the four ring areas. The variation of the β value demonstrated a greater effect on the mean value of the ESDI of RA3 during non-peak hours than during peak hours. The ESDI mean value of RA2 showed a slight downward tendency. The ESDI mean value of RA1 exhibited no noteworthy change in any case of β. The increasing β value resulted in the largest increase in the RSDI mean value in RA1, followed by RA2. The RSDI mean value of RA3 decreased with the increase in the β value. No obvious variation of the RSDI mean value of RA4 was observed.

Disaster management generally consists of four stages; disaster prevention, emergency response, recovery, and mitigation [61]. This research contributed to the first two stages by calculating the provision of shelter and rescue capabilities in megacities. Future urban planners and disaster managers could use the methods as a guide for disaster management, road network design, urban planning, and the improvement of disaster response capabilities.

This study attempted to develop SDIs to represent the supply and demand relationship of open spaces with a shelter function. This index was primarily characterized by the spatial interaction relationships of open spaces and the sites of evacuee or rescue facilities. It also reflected the space configuration for evacuation and rescue resources. The method presented in this study could help to identify weak areas and provide guidance for optimizing these areas. An ideal SDI value of 1 could be selected as a standard to evaluate the utilization of resources. Combined with the quadrant scatter plot figure and the spatial quadrant distribution map based on the ESDI values in the two traffic scenarios, the influence of traffic-restrictive factors on the effective utilization of each open space could be illustrated clearly. The two figures also helped in understanding the weak or strong areas in a city through the spatial clusters that emerged in the two figures.

Traffic jams should be cleared in the areas around the open spaces with high SDI values to contribute to sufficient usage of open spaces by accepting additional evacuees from distant communities. The transformation of subpar open spaces into suitable shelters around open spaces with low SDI values could be helpful in enhancing the security of nearby areas. In addition, considering various types of transportation (e.g., walking, riding the bus [62], or using special vehicles arranged by the government) for evacuation should be encouraged.

This study has several shortcomings that can be addressed in future works.

First, additional attraction factors should be included in addition to population, area, and service capabilities, used in this study, such as the preference of evacuees, the saturation of open spaces, or special demand from the disabled, the aged, or children.

Second, an accurate traffic simulation model should be further considered. Simulation models such as MATSim [63] could make this model realistic.

Third, the lack of real data to validate the reality and accuracy of the model makes this model theoretical; thus, further tests are required in the future.

6. Conclusions

This study measured the suitability of the spatial distribution of open spaces when they are used as post-disaster shelters, given that the Chinese government places increasing importance to urban safety. A CSDI based on the gravity model was constructed to evaluate the supply and demand relationship. The city of Wuhan in China was selected as the study area, and ESDI, RSDI, and CSDI were implemented to evaluate the evacuation and rescue capabilities of open spaces during peak and non-peak hours.

The following major conclusions are drawn from the analysis.

First, ESDI, RSDI, and CSDI can effectively evaluate the spatial suitability of open spaces when these models are integrated with the gravity model. The evaluation covers the travel time, capacity of open spaces, and service capability of rescue facilities. The effects of the distance-decaying function play an important role in the evaluation. Open spaces situated far from high-density communities or near the rescue facilities show a high ESDI or RSDI value.

Second, the quadrant distribution analysis of ESDI can be an effective method for revealing the reasons for the change in values in the two traffic scenarios and for helping planners to adjust their policies to enhance the capability of an area. The open spaces located in Quadrant I are sufficient to provide shelters. The open spaces located in Quadrants II and IV are affected by traffic conditions; thus, planners should aim to relieve traffic pressure around these areas. Considerable attention should be focused on the open spaces located in Quadrant III for monitoring and improving because these shelters are insufficient quantitatively. The indexes and the quadrant distribution analysis provided in this study can help planners to implement spatial layout evaluations of public facilities and support decision-making during facility optimization in urban planning.

Third, the impact of the different β values on SDIs shows positive, negative, and inconspicuous correlations with large, moderate, and minimal variations, respectively.

Fourth, the analysis of the supply–demand relationship of open spaces in Wuhan suggests a spatial mismatch in comprehensive evacuation and rescue capabilities. Open spaces in the central city were lacking in evacuation capability, whereas open spaces in the urban fringe could not obtain sufficient rescue opportunities. Several low values for the comprehensive evacuation and rescue capabilities of open spaces are scattered throughout the city.

Finally, traffic congestion can be a significant impact factor for evacuation and rescue capabilities but not on the comprehensive capability. This finding indicates that the integrated rational distribution of evacuation and rescue facilities can partially mitigate the impact of traffic congestion on the efficiency of disaster response. For shelter planning, measuring the suitable spatial supply–demand relationship is important.

Author Contributions: Yaolin Liu and Yanfang Liu conceived the study; Jie Gong and Pujiang Huang designed and performed the experiments; Jie Gong analyzed the data and wrote the paper; and Jiwei Li helped to revise paper and enhance its expression before submission.

References

1. Zhang, L.; Liu, X.; Li, Y.; Liu, Y.; Liu, Z.; Lin, J.; Shen, J.; Tang, X.; Zhang, Y.; Liang, W. Emergency medical rescue efforts after a major earthquake: Lessons from the 2008 wenchuan earthquake. *Lancet* **2012**, *379*, 853–861. [CrossRef]

2. Editing Group of Tangshan Earthquake. *Tangshan Earthquake on 1976*; Seismological Press: Beijing, China, 1982; pp. 7–10. (In Chinese)

3. The Survey of Blast of Ruihai Company. Available online: http://www.bh.gov.cn/html/bhxqzww/YY24845/2015-09-01/Detail_882444.htm (accessed on 28 September 2015). (In Chinese)

4. Lämmel, G.; Grether, D.; Nagel, K. The representation and implementation of time-dependent inundation in large-scale microscopic evacuation simulations. *Transp. Res. Part C Emerg. Technol.* **2010**, *18*, 84–98. [CrossRef]

5. Korhonen, T.; Hostikka, S.; Heliövaara, S.; Ehtamo, H. Fds+evac: An agent based fire evacuation model. *Pedestr. Evacuation Dyn. 2008* **2010**, 109–120.

6. Wood, N.J.; Schmidtlein, M.C. Anisotropic path modeling to assess pedestrian-evacuation potential from cascadia-related tsunamis in the US Pacific Northwest. *Nat. Hazards* **2012**, *62*, 275–300. [CrossRef]

7. Modali, N.K. Modeling Destination Choice and Measuring the Transferability of Hurricane Evacuation Patterns. Master's Thesis, Louisiana State University, Baton Rouge, LA, USA, 18 November 2004.

8. Wilmot, C.G.; Modali, N.; Chen, B. *Modeling Hurricane Evacuation Traffic: Testing the Gravity and Intervening Opportunity Models as Models of Destination Choice in Hurricane Evacuation*; FHWA/LA.06/407; Louisiana Transportation Research Center and Department of Civil and Environmental Engineering of Louisiana State University: Baton Rouge, LA, USA, September 2006.

9. Baker, E.J. *Hurricane Evacuation in the United States*; Pielke, R., Jr., Pielke, R., Sr., Eds.; Routledge: Abingdon, UK, 2000.

10. Lindell, M.K.; Kang, J.E.; Prater, C.S. The logistics of household hurricane evacuation. *Nat. Hazards* **2011**, *58*, 1093–1109. [CrossRef]

11. Mileti, D.S.; Sorensen, J.H.; O'Brien, P.W. Toward an explanation of mass care shelter use in evacuations. *Int. J. Mass Emerg. Disasters* **1992**, *10*, 25–42.

12. Whitehead, J.C. One million dollars per mile? The opportunity costs of hurricane evacuation. *Ocean Coast. Manag.* **2003**, *46*, 1069–1083. [CrossRef]

13. Wu, H.C.; Lindell, M.K.; Prater, C.S. Logistics of hurricane evacuation in hurricanes Katrina and Rita. *Transp. Res. Part F Traffic Psychol. Behav.* **2012**, *15*, 445–461. [CrossRef]

14. Dow, K.; Cutter, S.L. Emerging hurricane evacuation issues: Hurricane Floyd and south Carolina. *Nat. Hazards Rev.* **2002**, *3*, 12–18. [CrossRef]

15. Riad, J.K.; Norris, F.H.; Ruback, R.B. Predicting evacuation in two major disasters: Risk perception, social influence, and access to resources 1. *J. Appl. Soc. Psychol.* **1999**, *29*, 918–934. [CrossRef]

16. Musharraf, M.; Smith, J.; Khan, F.; Veitch, B.; MacKinnon, S. Assessing offshore emergency evacuation behavior in a virtual environment using a bayesian network approach. *Reliab. Eng. Syst. Saf.* **2016**, *152*, 28–37. [CrossRef]

17. Lindell, M.K.; Lu, J.C.; Prater, C.S. Household decision making and evacuation in response to hurricane lili. *Nat. Hazards Rev.* **2005**, *6*, 171–179. [CrossRef]

18. Saha, S.K.; James, H. Reasons for non-compliance with cyclone evacuation orders in Bangladesh. *Int. J. Disaster Risk Reduct.* **2017**, *21*, 196–204. [CrossRef]

19. Baker, E.J. Hurricane evacuation behavior. *Int. J. Mass Emerg. Disasters* **1991**, *9*, 287–310.

20. Gharakhlou, M.; Sabokbar, F. Access enhancement by making changes in the route network to facilitate rescue operations in urban disasters. *Int. J. Environ. Res.* **2010**, *4*, 183–192.

21. Sun, J.; Zhu, X.; Zhang, C.; Fang, Y. Rescueme: Location-based secure and dependable vanets for disaster rescue. *IEEE J. Sel. Areas Commun.* **2011**, *29*, 659–669. [CrossRef]

22. Kleiner, A.; Brenner, M.; Bräuer, T.; Dornhege, C.; Göbelbecker, M.; Luber, M.; Prediger, J.; Stückler, J.R.; Nebel, B. Successful search and rescue in simulated disaster areas. *Lect. Notes Comput. Sci.* **2006**, *4020*, 323–334.

23. Barbarosoğlu, G.; Arda, Y. A two-stage stochastic programming framework for transportation planning in disaster response. *J. Oper. Res. Soc.* **2004**, *55*, 43–53. [CrossRef]

24. Hu, Z.H.; Sheng, Z.H. Disaster spread simulation and rescue time optimization in a resource network. *Inf. Sci.* **2015**, *298*, 118–135. [CrossRef]

25. Wei, X.; Lv, W.; Song, W. Rescue route reselection model and algorithm for the unexpected accident. *Procedia Eng.* **2013**, *62*, 532–537. [CrossRef]

26. D'Agostino, F.; Farinelli, A.; Grisetti, G.; Iocchi, L. Monitoring and information fusion for search and rescue operations in large-scale disasters. In Proceedings of the International Conference on Information Fusion, Washington, DC, USA, 8–11 July 2002; Volume 671, pp. 672–679.

27. Khamis, N.; Misfian, A.M.; Md Noor, R. Towards sustainable software criteria: Rescue operation and disaster management system model. In Proceedings of the ICNSC IEEE International Conference on Networking, Sensing and Control, Evry, France, 10–12 April 2013; pp. 398–403.

28. Barsky, L.E.; Trainor, J.E.; Torres, M.R.; Aguirre, B.E. Managing volunteers: Fema's urban search and rescue programme and interactions with unaffiliated responders in disaster response. *Disasters* **2007**, *31*, 495–507. [CrossRef] [PubMed]

29. Burby, R.J.; Beatley, T.; Berke, P.R.; Deyle, R.E.; French, S.P.; Godschalk, D.R.; Kaiser, E.J.; Kartez, J.D.; May, P.J.; Olshansky, R. Unleashing the power of planning to create disaster-resistant communities. *J. Am. Plan. Assoc.* **1999**, *65*, 247–258. [CrossRef]

30. Glavovic, B.C.; Saunders, W.S.A.; Becker, J.S. Land-use planning for natural hazards in New Zealand: The setting, barriers, 'burning issues' and priority actions. *Nat. Hazards* **2010**, *54*, 679–706. [CrossRef]

31. Acharya, G.; Bennett, L.L. Valuing open space and land-use patterns in urban watersheds. *J. Real Estate Financ. Econ.* **2001**, *22*, 221–237. [CrossRef]

32. Cho, S.H.; Lambert, D.M.; Kim, S.G.; Roberts, R.K.; Park, W.M. Relationship between value of open space and distance from housing locations within a community. *J. Geogr. Syst.* **2011**, *13*, 393–414. [CrossRef]

33. Jiao, L.; Liu, Y. Geographic field model based hedonic valuation of urban open spaces in Wuhan, China. *Landsc. Urban Plan.* **2010**, *98*, 47–55. [CrossRef]

34. Nicol, C.; Blake, R. Classification and use of open space in the context of increasing urban capacity. *Plan. Pract. Res.* **2000**, *15*, 193–210. [CrossRef]

35. Van Herzele, A.; Wiedemann, T. A monitoring tool for the provision of accessible and attractive urban green spaces. *Landsc. Urban Plan.* **2003**, *63*, 109–126. [CrossRef]

36. Wu, J.; Plantinga, A.J. The influence of public open space on urban spatial structure. *J. Environ. Econ. Manag.* **2003**, *46*, 288–309. [CrossRef]

37. Rossano, L. Hyogo framework for action 2005–2015: Building the resilience of nations and communities to disasters. In Proceedings of the World Conference on Disaster Reduction, Kobe, Japan, 18–22 January 2005.

38. China Seismological Bureau. *Standards of Earthquake Emergency Shelter and Related Facilities*; China Seismological Bureau: Beijing, China, 2008. (In Chinese)

39. The Planning of Comprehensive Disaster Prevention and Shelter in the Wuhan Urban Development Area. Available online: http://www.wpdi.cn/nry.aspx?pageid=14&menuid=16 (accessed on 20 December 2014). (In Chinese)

40. Ministry of Civil Affairs of the People's Republic of China. *The Promotion of Constructing of Urban Community Across the Country*; Ministry of Civil Affairs of the People's Republic of China: Beijing, China, 2000. (In Chinese)

41. What is the Principle of Dividing the Community? Available online: http://www.hbmzt.gov.cn/sqmy/201103/t20110318_95296.shtml (accessed on 5 May 2017). (In Chinese)

42. Tianjin Construction Management Committee. *Standard for Public Facilities of Urban Residential District of Tianjin*; Tianjin Construction Management Committee: Tianjin, China, 2008. (In Chinese)

43. Hangzhou Planning Bureau. *Supporting Regulations for Public Service Facilities in Urban Planning of Hangzhou*; Hangzhou Planning Bureau: Hangzhou, China, 2009. (In Chinese)

44. Qingdao Planning Bureau. *Sandard and Guideline for Public Service Facilities in Urban Planning of Qingdao*; Qingdao Planning Bureau: Qingdao, China, 2010. (In Chinese)

45. Chongqing Planning Bureau. *Guidelines for Public Service Facilities in Urban and Rural Planning of Chongqing*; Chongqing Planning Bureau: Chongqing, China, 2008. (In Chinese)

46. Chongqing Planning Bureau. *Standard for Public Service Facilities Setting in Residential Area of Chongqing*; Chongqing Planning Bureau: Chongqing, China, 2005. (In Chinese)

47. Wuhan Transport Survey Weekly. Available online: http://www.whtpi.com/News/11.html (accessed on 5 May 2014). (In Chinese)

48. Zhang, Y.; Zheng, L.; Gao, J. Earthquake prevention planning: A case study of Xichang. *Plan. Forum* **2011**, *27*, 19–25. (In Chinese)

49. Higgs, G.; Fry, R.; Langford, M. Investigating the implications of using alternative GIS-based techniques to measure accessibility to green space. *Environ. Plan. B Plan. Des.* **2012**, *39*, 326–343. [CrossRef]

50. Boone, C.G.; Buckley, G.L.; Grove, J.M.; Sister, C. Parks and people: An environmental justice inquiry in Baltimore, Maryland. *Ann. Assoc. Am. Geogr.* **2009**, *99*, 767–787. [CrossRef]

51. La Rosa, D. Accessibility to greenspaces: GIS based indicators for sustainable planning in a dense urban context. *Ecol. Indic.* **2014**, *42*, 122–134. [CrossRef]

52. Geza, T. The application of gravity model in the investigation of spatial structure. *Acta Polytech. Hung.* **2014**, *11*, 5–19.

53. Crooks, V.A.; Schuurman, N. Interpreting the results of a modified gravity model: Examining access to primary health care physicians in five Canadian provinces and territories. *BMC Health Serv. Res.* **2012**, *12*, 230. [CrossRef] [PubMed]

54. White, N.; Mengersen, K. Predicting health programme participation: A gravity-based, hierarchical modelling approach. *J. R. Stat. Soc.* **2016**, *65*, 145–166. [CrossRef]

55. Yao, J.; Murray, A.T.; Agadjanian, V. A geographical perspective on access to sexual and reproductive health care for women in rural Africa. *Soc. Sci. Med.* **2013**, *96*, 60–68. [CrossRef] [PubMed]

56. Chang, H.S.; Liao, C.-H. Exploring an integrated method for measuring the relative spatial equity in public facilities in the context of urban parks. *Cities* **2011**, *28*, 361–371. [CrossRef]

57. Omer, I. Evaluating accessibility using house-level data: A spatial equity perspective. *Comput. Environ. Urban Syst.* **2006**, *30*, 254–274. [CrossRef]

58. McGrail, M.R.; Humphreys, J.S. Measuring spatial accessibility to primary care in rural areas: Improving the effectiveness of the two-step floating catchment area method. *Appl. Geogr.* **2009**, *29*, 533–541. [CrossRef]

59. Luo, W.; Wang, F. Measures of spatial accessibility to health care in a GIS environment: Synthesis and a case study in the Chicago region. *Environ. Plan. B Plan. Des.* **2003**, *30*, 865–884. [CrossRef]

60. Saaty, T.L. How to make a decision: The analytic hierarchy process. *Eur. J. Oper. Res.* **1990**, *48*, 9–26. [CrossRef]

61. Zhou, M.; Fan, Y.D.; Yang, S.Q. *Natural Disaster Risk Management and Early Warning System*; Science Press: Beijing, China, 2010; pp. 20–25. (In Chinese)

62. Bish, D.R. Planning for a bus-based evacuation. *OR Spectr.* **2011**, *33*, 629–654. [CrossRef]

63. Agent-Based Transport Simulations Matsim. Available online: http://www.matsim.org/ (accessed on 13 November 2016).